Eddy Currents in an Infinitely Finely Segmented Hall Generator

E. S. Jett,* D. L. Denzel,† and Y. C. L. Wu‡
The University of Tennessee Space Institute, Tullahoma, Tenn.

The eddy currents in the cross-sectional plane of a conducting side wall Hall generator are studied. Fluid velocity and temperature effects are investigated by assuming two different types of flow, i.e., fully developed laminar flow and turbulent boundary-layer flow. The working fluid is a seeded combustion gas where the compositions were calculated by assuming chemical equilibrium. The electrical conductivity and Hall parameter are allowed to vary as functions of temperature and pressure, and their values are calculated based on approximations formulated by Frost. Cold and hot channel wall conditions reveal quite different current distributions under laminar, fully developed flow conditions, with the cold wall distribution being much more nonuniform. Under turbulent boundary-layer flow conditions, however, cold and hot wall current distributions exhibit relatively minor differences, with both cases approaching the limiting case of constant velocity and electrical properties. Increasing the magnetic field strength and Hall parameter tends to increase the nonuniformity of the current distribution. The power output of the Hall generator is shown to depend strongly on the wall temperature under laminar, fully developed flow conditions, but this dependence is greatly reduced when the turbulent boundary-layer velocity profile is assumed.

Introduction

EXPERIMENTAL work conducted by the MHD research group at The University of Tennessee Space Institute using a copper-walled MHD Hall generator, as illustrated in Fig. 1, had shown that a large fraction of the current was flowing to the side walls of the generator.[1] The flowing of part of the current to the side walls of the generator was not particularly surprising in itself. However, the effect had not been previously noted since most of the experimental work in MHD power generator has used channels with nonconducting walls parallel to the magnet pole faces. This work, then, is an attempt to theoretically verify the aforementioned effect and determine the effects of the side wall currents on generator behavior.

The current distribution in MHD channels has been studied quite completely for certain conditions. Since the three-dimensional current distribution problem has not been solved, most studies so far have chosen one of two planes for a two-dimensional investigation. A plane parallel to the axial coordinate would be chosen in order to study the current distribution along the channel, where finite electrode segmentation may be included. Examples of this kind of study include those by Celenski and Fischer,[2] and Oliver.[3]

However, this particular study is concerned with the cross-sectional current distribution, so a plane perpendicular to the axial coordinate is chosen. Important early work in the cross-sectional plane of MHD channels was performed by Shercliff,[4] who considered the fully developed, incompressible flow of a viscous, electrically conducting fluid through a rectangular channel with nonconducting walls. The electrical conductivity of the fluid was assumed to be constant, and the Hall effect was not included. He found that for sufficiently high applied magnetic field the flowfield became a core of uniform flow surrounded by boundary layers on each wall. By some additional reasoning, he was able to extend the solution to channels of any symmetric cross-sectional shape.

In later work, Shercliff[5] considered circular channels with conducting walls. Following a procedure similar to that used in his earlier paper,[4] Shercliff again found a core region and a boundary-layer region in the flow. The current density in the core region was found to be uniform and in the direction of the induced electric field, perpendicular to both the applied magnetic field and the direction of fluid flow. The current loops were completed by the current returning in the boundary layer and wall.

Tani[6] used a minimum principle to develop an approximate solution for MHD flow through rectangular channels. However, the method can be extended to arbitrary cross-sectional shape. He considered cases both where all walls are electrically nonconducting, and where a pair of the walls is nonconducting while the other pair is electrically conducting. Constant electrical conductivity in the fluid was assumed and the Hall effect was included for small Hall parameter. He found that the inclusion of the Hall effect produced a cross flow in the fluid with a double swirl pattern.

Chang and Lundgren,[7] also assuming constant conductivity, solved the rectangular duct flow problem where the walls are conductors. They found that increasing the wall conductivity tends to decrease the average velocity of the fluid. They also found a solution for flow in arbitrary symmetrical channels, and improved upon Shercliff's solution[5] by not restricting the wall conductivity to be small. Their results for perfectly conducting walls and a large Hartmann

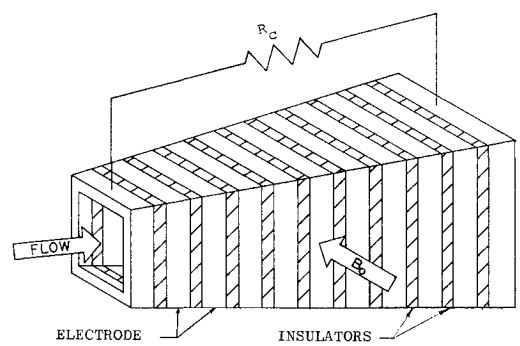

Fig. 1 Hall generator configuration.

Received September 11, 1969; revision received February 24, 1970. Work was sponsored by the Air Force Office of Scientific Research, Office of Aerospace Research, U.S. Air Force, under Contract F44620-69-C-0031.

* Graduate Research Assistant; present address General Dynamics, Fort Worth, Texas.
† Assistant Professor, Electrical Engineering.
‡ Associate Professor, Aerospace Engineering. Member AIAA.

number were similar to Shercliff's results for walls of small conductivity in that the velocity tends to be uniform except in a thin boundary-layer region.

Carlson[8] proposed a Hall generator with nonconducting walls but with wire electrodes extending entirely across the channel. The wires lie in one or more planes perpendicular to the applied magnetic field, each wire being perpendicular to the direction of fluid flow. Constant conductivity and Hall parameter were assumed in addition to the assumption of uniform velocity. He found that the performance of the generator was dependent on the value of the Hall parameter. The current was found to flow from one end of the wire electrode, through the fluid, and back into the other end of the electrode.

Hughes and Young[9] give a good summary of work in the cross-sectional plane of rectangular and circular channels, showing current and velocity distributions for different channel configurations. All cases shown, however, are under the assumptions of constant electrical conductivity and negligible Hall effect.

More recently Lengyel[10] studied the current distribution in both the xy plane and yz plane for a Faraday generator. He considered a fully developed laminar flow with non-equilibrium ionization.

Formulation of the Problem

An exact solution of the problem would require the simultaneous solution of the electromagnetic equations, i.e., Ohm's law and the Maxwell relations, together with the fluid dynamic equations with the induced Lorentz force as a body force and joule heating as a heat addition term. In order to avoid this highly complex situation, it is assumed that the MHD forces have a negligible effect on the fluid flow, which effectively drops the electro-magnetic terms out of the fluid dynamic equations. This assumption restricts the solution to be valid only for small interaction parameters. Thus the fluid dynamic equations, uncoupled from the electromagnetic equations, may be solved independently.

The geometry of the problem is illustrated in Fig. 2. Additional assumptions are as follows: 1) steady state; 2) no variation of properties in the axial direction, i.e., $\partial/\partial x = 0$ (this assumption also implies infinitely fine electrode segmentation, so that no current concentration occurs on the electrode edges or in the channel); 3) small magnetic Reynolds number, so that the induced magnetic field is much smaller than the applied one and can be neglected.

The problem as formulated is governed by electromagnetic equation only with known fluid properties, since the fluid dynamic equations are assumed to be decoupled from the electromagnetic equations.

The first governing equation is the generalized Ohm's law, which relates the current density vector $\mathbf{j}$ to the electric field vector $\mathbf{E}$. It may be written

$$\mathbf{j} = \sigma(\mathbf{E} + \mathbf{V} \times \mathbf{B}) - (\Omega/|\mathbf{B}|)(\mathbf{j} \times \mathbf{B}) \quad (1)$$

where $\mathbf{B}$ is the magnetic field vector, $\mathbf{V}$ is the fluid velocity vector, σ is the electrical conductivity of the fluid, and Ω is the Hall parameter.

The other governing equations include the conservation of current density

$$\nabla \cdot \mathbf{j} = 0 \quad (2)$$

which comes from one of the Maxwell relations, and

$$\nabla \times \mathbf{E} = 0 \quad (3)$$

which expresses the irrotationality of the electric field.

Ohm's Law may be written in component form, giving the current densities in the three space coordinate directions;

$$j_x = [\sigma/(1 + \Omega^2)][(E_x - vB_0) + \Omega(E_y + uB_0)] \quad (4)$$

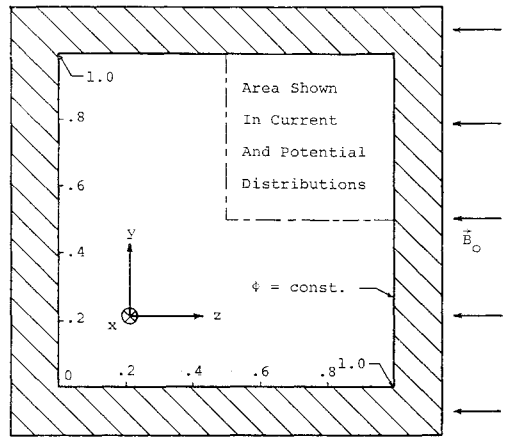

Fig. 2 Channel element in the cross-sectional plane.

$$j_y = [\sigma/(1 + \Omega^2)][(E_y + uB_0) - \Omega(E_x - vB_0)] \quad (5)$$

$$j_z = \sigma E_z \quad (6)$$

where $\mathbf{B} = -B_0\mathbf{k}$ and B_0 is the constant applied magnetic field.

Expanding Eq. (2), recalling that $\partial/\partial x = 0$, results in

$$\frac{\partial j_y}{\partial y} + \frac{\partial j_z}{\partial z} = 0 \quad (7)$$

Thus, a current function ψ can be defined for the two current density components j_y and j_z

$$j_y = \partial\psi/\partial z \text{ and } j_z = -\partial\psi/\partial y \quad (8)$$

From Eq. (3) and the assumption of $\partial/\partial x = 0$, we have

$$\partial E_z/\partial y - \partial E_y/\partial z = 0 \quad (9)$$

and

$$\partial E_x/\partial y = \partial E_x/\partial z = \partial E_x/\partial x = 0 \quad (10)$$

Equation (10) gives the important result that E_x is constant.

Equation (9) allows the introduction of a scalar potential φ defined by

$$E_y = -\partial\varphi/\partial y,\ E_z = -\partial\varphi/\partial z$$

A partial differential equation in φ can be obtained by allowing σ, Ω, u, and v to be functions of y and z, and eliminating $\mathbf{j}$ from the Ohm's Law by Eq. (7). The following equation is obtained after some rearrangement:

$$\frac{\partial^2\varphi}{\partial y^2} + (1 + \Omega^2)\frac{\partial^2\varphi}{\partial z^2} + \frac{\partial \ln\sigma}{\partial y}\frac{\partial\varphi}{\partial y} + (1 + \Omega^2)\frac{\partial \ln\sigma}{\partial z}\frac{\partial\varphi}{\partial z} + [\Omega(E_x - vB_0) - uB_0]\frac{\partial \ln\sigma}{\partial y} - B_0\frac{\partial u}{\partial y} + E_x\frac{\partial\Omega}{\partial y} - B_0\left(\Omega\frac{\partial v}{\partial y} + v\frac{\partial\Omega}{\partial y}\right) + \frac{2\Omega\partial\Omega/\partial y}{1 + \Omega^2} \times \left[uB_0 - \frac{\partial\varphi}{\partial y} - \Omega(E_x - vB_0)\right] = 0 \quad (11)$$

This equation must be solved for φ within the region bounded by the four walls of the MHD channel. The boundary condition for Eq. (11) is that the potential φ is constant on the surrounding walls, since the walls are assumed to be perfect electrical conductors.

Thus, the problem is now reduced to solving Eq. (11) by providing E_x and B_0, which are both constants, along with distributions for $\Omega(y,z)$, $\sigma(y,z)$, $u(y,z)$, and $v(y,z)$. Different distributions of these properties will be assumed in order to simulate different generator operating conditions.

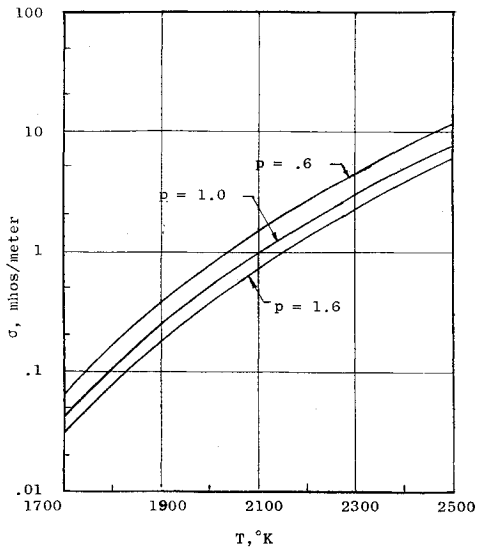

Fig. 3 Variation of conductivity with temperature at various pressures for a potassium seeded (1% by wt) combustion gas.

The result will be a distribution of $\varphi(y,z)$ corresponding to the operating conditions implied by the property distributions. This will allow the calculation of $(\partial\varphi/\partial y)$ and $(\partial\varphi/\partial z)$ which along with the property distributions may in turn be used to obtain distributions of the current density.

The total available generator current i is the integral of the Hall current j_x when the generator is connected as a Hall generator. Thus, i can be found as a function of j_x by integrating j_x over the cross-sectional area, as

$$i = \int A j_x dy dz \tag{12}$$

Velocity Distributions and Fluid Properties

Because of the presence of velocity, conductivity, and Hall parameter terms in the differential equation in Eq. (11), the velocity and other fluid property distributions in the channel must be given. It will now be assumed that only the axial component of velocity is of importance. Thus, v and $\partial v/\partial y$ drop out of the equations. Two cases for the distribution of $u(y,z)$ have been considered: fully developed laminar flow and turbulent boundary-layer flow.

The velocity distribution used for the laminar case is a standard solution for laminar flow in a finite rectangular duct. As given by Rouse,[11] the distribution in terms of y and z is

$$u(y,z) = \frac{1}{2\mu}\frac{\partial p}{\partial x} y(y-d) + \sum_{m=1}^{\infty} \sin\frac{m\pi y}{d} \times \left(A_m \cosh\frac{m\pi z}{d} + B_m \sinh\frac{m\pi z}{d}\right) \tag{13}$$

where μ is the fluid viscosity, p is the pressure, and the coefficients A_m and B_m are given by

$$A_m = -(2d^2/\mu m^3\pi^3)(\partial p/\partial x)(\cos m\pi - 1),$$
$$B_m = -A_m(\cosh mn\pi - 1)/\sinh mn\pi$$

where $n = d/b$, the aspect ratio of the channel. The choice of fully developed flow for the laminar case is mathematically consistent with the assumption of $\partial/\partial x = 0$. The average velocity corresponding to the fully developed laminar flow case may be found by integrating Eq. (13).

In practice, it was found that allowing the summations in Eq. (13) to end at $m = 5$ was sufficient, and carrying the summations to values of m greater than five brought on some numerical difficulties.

The most commonly used profile for the turbulent boundary layer is of the form

$$u(y)/u_\infty = (y/\Delta)^{1/7} \tag{14}$$

where Δ is the boundary-layer thickness, y is the distance from the wall, and u_∞ is the velocity in the inviscid region of the flowfield. Although this profile actually applies for flow over a flat plate, it will be considered that by applying the expression at all four walls, a reasonable approximation of channel flow with turbulent boundary layer on the walls can be obtained.

The electrical conductivity and the Hall parameter are calculated for the mixture of combustion gas and potassium hydroxide[12] using the approximate method from Frost.[13] The chemical reactions are assumed to be in equilibrium. A thermodynamic property table including the electron mobility and conductivity can then be calculated for specific combustion chamber conditions.

Figure 3 shows plots of conductivity of a combustion gas seeded with KOH (1% K by weight) as a function of temperature for various pressures. The conductivity decreases drastically in the lower part of the temperature range. Figure 4 illustrates the Hall parameter as a function of temperature for several values of pressure. The variation is quite linear in the temperature range of interest.

The relation between velocity and enthalpy is assumed to obey the Crocco integral

$$u/u_\infty = (H - H_w)/(H_\infty - H_w)$$

where H is the total enthalpy, defined by $H = h + \frac{1}{2}u^2$, where h is the static enthalpy. The subscript ∞ refers to conditions at the axial centerline of the channel, whereas the subscript w refers to values at the wall. Knowing the velocity distribution in the cross section of the channel, we can determine the static enthalpy which in turn will determine the temperature distribution in the channel using the thermodynamic chart mentioned above (the pressure in the cross section must be specified).

Results and Discussion

Throughout the presentation of results, the term "hot wall" will refer to conditions where the wall temperature is 2500°K. "Cold wall" will imply a wall temperature of 1700°K. The prescribed centerline temperature T_∞ is always 2500°K.

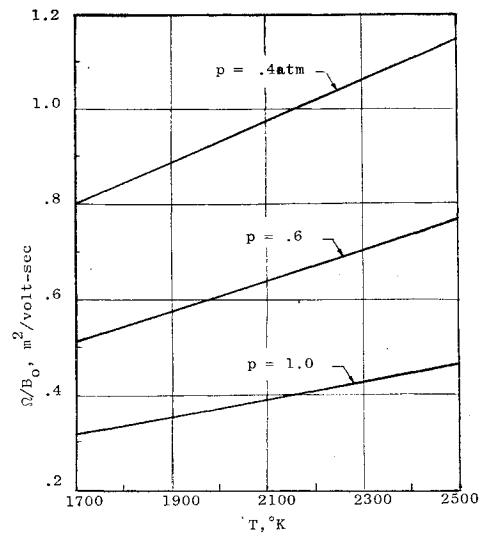

Fig. 4 Variation of Hall parameter with temperature at various pressures for a potassium seeded (1% by weight) combustion gas.

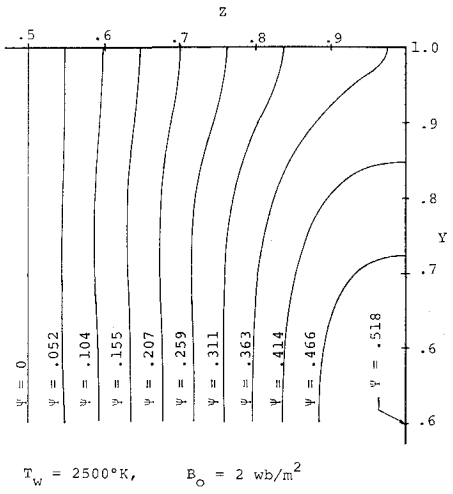

Fig. 5 Current distribution for short circuit, hot wall, fully developed laminar flow conditions.

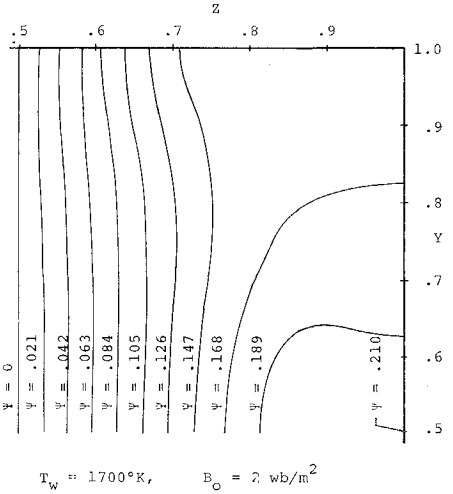

Fig. 7 Current distribution for short circuit, cold wall fully developed laminar flow conditions.

The terms "short circuit" and "open circuit" refer to the electrical loading of the generator. Under short circuit conditions, the load resistance of the generator is zero, thus E_x is also zero. On the other hand, the load resistance is infinite under open circuit conditions, and the total current is zero. Normally, a generator is operated at conditions somewhere between short and open circuit, since power cannot be removed at either open or short circuit. However, it is reasonable to expect that the current distribution for any electrical loading condition will fall somewhere between the distributions at open and short circuit.

With reference to velocity conditions, "laminar" refers to the assumed fully developed laminar distribution. A "thick" boundary layer implies that the boundary-layer thickness Δ is equal to one-fourth of the channel height on the electrode walls and one-fourth of the channel width on the side walls, while a "thin" boundary layer means that Δ was reduced to one-tenth of the channel dimensions. In all cases, the average velocity of the fluid was prescribed to be 1500 m/sec. The channel cross section was a square. The pressure was assumed to be 1 atm.

In the results presented below, the magnetic field strength was taken to be 2 webers/m^2 unless otherwise noted.

The working fluid was a mixture of combustion gas seeded with potassium hydroxide. The electron mobility and electrical conductivity of the gas are shown in Figs. 3 and 4, respectively.

Figure 5 illustrates the current stream function distribution for a laminar, hot wall, short circuit case. The distribution is seen to be fairly homogeneous. That is, there are no regions of extremely high or extremely low current density, as would be indicated by the distance between the streamlines. This homogeneity is to be expected in this and all other hot wall cases since the variation of conductivity is quite small. It may be seen that a significant portion of the current, just under 30%, is flowing to the side wall of the channel.

The open circuit distribution for the hot wall laminar case is shown in Fig. 6. It is quite similar to the short circuit case, with somewhat less current flowing to the side wall.

The laminar, cold wall, short circuit case is shown in Fig. 7, and is seen to be much less uniform than the hot wall cases. The layer of low conductivity on the side wall has forced most of the current flow to the center region of the channel. There is also a region of low conductivity along the top and bottom walls, but these have relatively little effect on the cross-sectional current distribution, since the current flows primarily in a vertical direction because of the $\mathbf{V} \times \mathbf{B}$ induced electric field. The current density along the side wall and in the corner region is seen to be quite low. In contrast, the current density near the vertical centerline of the channel is quite high.

Figure 8 illustrates the corresponding open circuit case, which again is highly nonuniform. However, a new effect has appeared. Some of the current flowing to the side wall

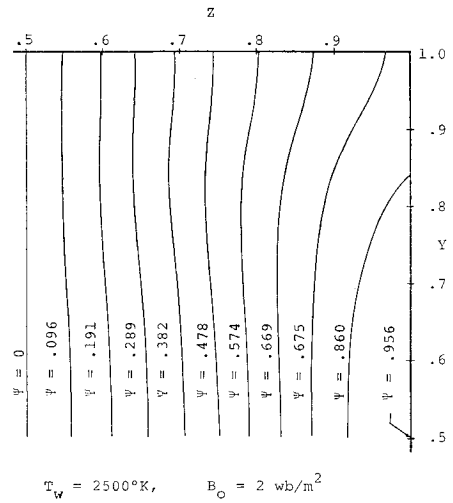

Fig. 6 Current distribution for open circuit, hot wall, fully developed laminar flow conditions.

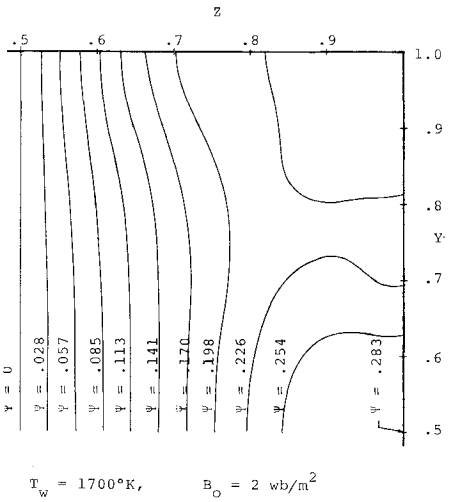

Fig. 8 Current distribution for open circuit, cold wall, fully developed laminar flow conditions.

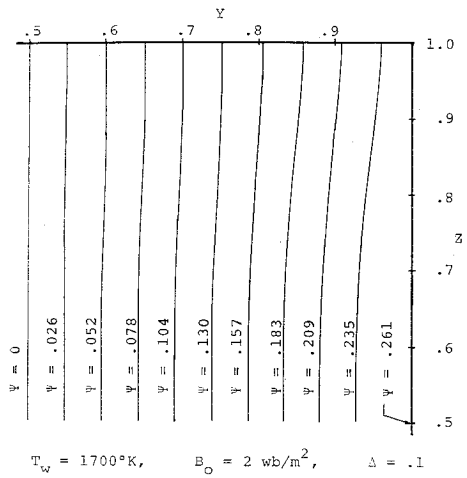

Fig. 9 Current distribution for short circuit, cold wall, thin turbulent boundary-layer flow conditions.

is returning from the side wall to flow to the top wall, setting up current loops between the side and top walls. These current loops have also been shown to exist for a finite conducting wall by Bitiurin et al.[14]

In the case of turbulent flow, the current distribution is much more uniform regardless of the wall temperature, boundary-layer thickness, and short or open circuits conditions. Figure 9 shows the current distribution for a cold wall (T_w = 1700°K), thin turbulent boundary-layer flow operated at short circuit condition.

When the Hall parameter is increased, more nonuniformity in the current distribution results. This is especially so for the cold wall laminar flow condition.

Figure 10 shows the equipotential lines in the upper right quadrant of the channel cross section for a cold wall, thin turbulent boundary layer flow at short circuit conditions. The potential gradients are much larger near the electrode than at the side walls. This situation is generally true for all conditions except that of the cold wall, fully developed laminar flow. In that case the potential gradients are large near both the electrodes and the side walls.

The voltage-current characteristics have been plotted for several cases and compared so that the effects of wall temperature and velocity distribution on the power generating capability of MHD channels operating under various conditions may be noted. Figure 11 shows load lines for hot and cold wall laminar flow, hot and cold wall turbulent flow where the thick boundary layer is assumed, and flow with

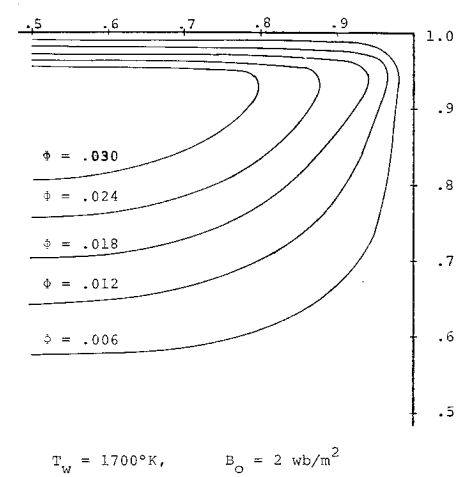

Fig. 10 Cross-sectional potential distribution for short circuit, cold wall, thick turbulent boundary-layer flow conditions.

constant velocity and electrical properties. The results for the thin turbulent boundary layer are not shown since they are very nearly the same as the corresponding results for the thick boundary layer.

The highest power output is produced by the laminar, hot wall case. On the other hand, the laminar, cold wall case produced the lowest power output. The great difference in the two cases indicates the importance of the conductivity difference between hot and cold wall laminar flow. In the hot wall case, where the wall temperature is equal to T_∞, a temperature overshoot effect causes a rise in the temperature between the wall and the axial centerline. Thus, the average conductivity would be higher than the value of the conductivity corresponding to T_∞. In the cold wall case, T_w is sufficiently lower than T_∞ so that the average conductivity in the cold wall, laminar case would be significantly below the conductivity corresponding to T_∞. This conductivity difference is evidently a major cause of the difference in power output of hot and cold wall operating conditions in the laminar flow case. However, other effects, such as a difference in the Hall parameter as a result of the temperature difference, undoubtedly enter in. The significance of other effects is not as clear as is the importance of the conductivity difference.

The power output for the hot and cold wall, thick turbulent boundary-layer cases, and for the case of constant velocity and properties ($u = \bar{u}$, $\sigma = \sigma_\infty$, and $\Omega = \Omega_\infty$ were used) are all quite similar. This result is consistent with a similar result noted with respect to the current and potential distributions, and has the same apparent cause. That is the nature of the $\frac{1}{7}$ power velocity profile is such that most of the temperature gradient takes place near the wall, so that the region of variable conductivity is small.

Figure 12 shows the comparison of the theoretical result and experiment.[1] The two end segments of the electrode were connected with the side walls in the experiments (see Fig. 20 of Ref. 1). Therefore, the current flows into these two end pieces include the side wall current. The two theoretical results correspond to cold wall (T_w = 1700°K) turbulent boundary layer and short circuit condition. One is for a freestream Hall parameter of approximately 1, the other is for about 3. The low Hall parameter result corresponding to the experimental condition gives a much uniform

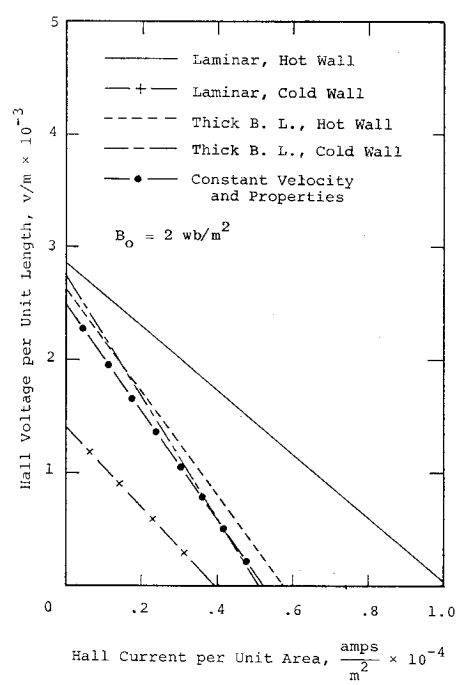

Fig. 11 Voltage-current characteristics of Hall generator.

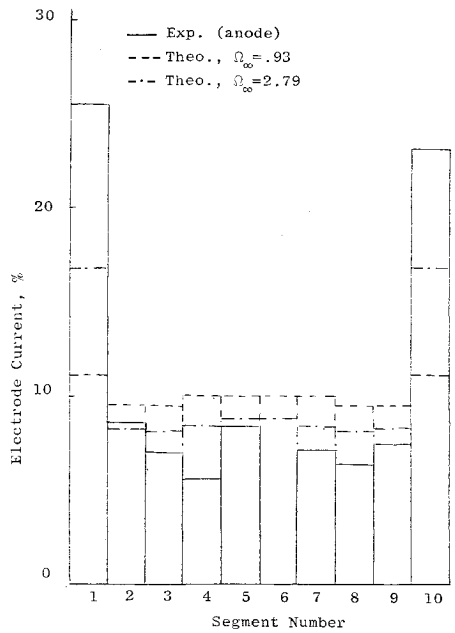

Fig. 12 Current distribution on electrode and side walls (segments 1 and 10 are connected with the side wall).

current distribution. The high Hall parameter case compares much more favorably with the experiment. The improved agreement is due to the fact that the change of the Hall parameter has similar effect as change of the cross-sectional aspect ratio. This can be easily seen by nondimensionalizing Eq. (11).

Let $\eta = y/d$, $\xi = z/b$, $\Phi = \varphi/\bar{u}B_0d$, $U = u/\bar{u}$, $V = v/\bar{u} = 0$ is assumed throughout the calculations and $\bar{E}_x = E_x/\bar{u}B_0$ where d is the distance between electrodes and b the distance separating the side walls, B_0 the applied magnetic field and $\bar{u}$ the average velocity. Equation (11) becomes

$$\frac{\partial^2\Phi}{\partial\eta^2} + \left[\frac{d^2}{b^2}(1+\Omega^2)\right]\frac{\partial^2\Phi}{\partial\xi^2} + \frac{\partial \ln\sigma}{\partial\eta}\frac{\partial\Phi}{\partial\eta} + \left[\frac{d^2}{b^2}(1+\Omega^2)\right]\frac{\partial \ln\sigma}{\partial\xi}\frac{\partial\Phi}{\partial\xi} + (\Omega\bar{E}_x - U)\frac{\partial \ln\sigma}{\partial\eta} - \frac{\partial U}{\partial\eta} - \bar{E}_x\frac{\partial\Omega}{\partial\eta} + \frac{\partial \ln[(d^2/b^2)(1+\Omega^2)]}{\partial\eta}\left(U - \frac{\partial\Phi}{\partial\eta} - \Omega\bar{E}_x\right) = 0 \quad (15)$$

At short circuit conditions, $\bar{E}_x = 0$, then the change of channel cross section aspect ratio is almost equivalent to the change of the Hall parameter. In the experiment, the current distribution is measured at the No. 34 electrode which corresponds to $d = 5.05$ in. and $b = 2$ in., thus $(d/b)^2 = 6.4$. The low Hall parameter case corresponds to $\Omega_{l\infty} = 0.93$ and the high Hall parameter case corresponds to $\Omega_{h\infty} = 2.79$. Thus, we have $(1 + \Omega_{h\infty}^2) = 8.8$ and $(d/b)^2(1 + \Omega_{l\infty}^2) = 12$. Therefore, the high Hall parameter case simulates closer to the channel geometry and consequently yields better agreement. Furthermore, the experiment was conducted at a much lower wall temperature (approximately 600°K) than the wall temperature used in the computation ($T_w = 1700$°K). This difference will make the current less concentrated in the theoretical results.

Conclusion

The wall temperature has a very significant effect on the current and potential distributions and on the power output for the laminar, fully developed flow conditions. When the turbulent boundary-layer velocity profile is assumed, however, the difference between the wall and freestream temperatures becomes much less important. This is due to the fact that in turbulent flow, temperatures approaching the freestream temperature are reached in regions quite close to the walls. The thickness of the turbulent boundary layer has little effect either on the current and potential distributions or the power output of the generator.

The value of the load resistance of the Hall generator seems to have a relatively minor effect on the current and potential distributions in the cross-sectional plane, when compared with other more significant effects. This is particularly true in the turbulent boundary-layer cases.

Increasing the strength of the magnetic field, Hall parameter and decreasing the channel cross sections aspect ratio b/d increase the nonuniformity of the current distribution, generally causing more current to flow to the side walls and more to return from the side walls and flow on to the top wall under laminar flow conditions. Again, the turbulent flow current distributions are altered much less than the laminar cases, though there is a notable increase in the amount of current flowing to the side walls.

References

[1] Wu, Y. C. L. et al., "Two-Terminal Connected Open Cycle MHD Generators," *Proceedings of the Ninth Symposium on Engineering Aspect of Magnetohydrodynamics*, The University of Tennessee Space Institute, Tullahoma, Tenn., April 1968.

[2] Celinski, Z. N. and Fischer, F. W., "Two-Dimensional Analysis of MHD Generators with Segmented Electrodes," IPP 3/26, Jan. 1965, Institute fur Plasmaphysik, Garching bei Munchen.

[3] Oliver, D. A., "Nonuniform Electrical Conduction in Magnetohydrodynamic Channels," Rept. 163, May 1967, Stanford University Institute for Plasma Research, Stanford, Calif.

[4] Shercliff, J. A., "Steady Motion of Conducting Fluids in Pipes Under Transverse Magnetic Fields," *Proceedings of the Cambridge Philosophical Society*, Vol. 49, 1953, pp. 136–144.

[5] Shercliff, J. A., "The Flow of Conducting Fluids in Circular Pipes Under Transverse Magnetic Fields," *Journal of Fluid Mechanics*, Pt. VI, Vol. 1, 1956, pp. 644–666.

[6] Tani, I., "Steady Flow of Conducting Fluids in Channels Under Transverse Magnetic Fields, With Consideration of Hall Effect," *Journal of the Aerospace Sciences*, Vol. 29, No. 3, March 1962, pp. 297–305.

[7] Chang, C. C. and Lundgren, T. S., "Duct Flow in Magnetohydrodynamics," *Journal of Applied Mathematics and Physics*, (ZAMP), Vol. 41, No. 12, 1961, pp. 100–114.

[8] Carlson, A. W., "A Hall Generator with Wire Electrodes," BSD-TDR-63-196, Sept. 1963, Avco-Everett Research Lab., Everett, Mass.

[9] Hughes, W. F. and Young, F. J., *The Electromagnetodynamics of Fluids*, Wiley, New York, 1966.

[10] Lengyel, L. L., "Two-Dimensional Current Distributions in Faraday Type MHD Energy Converters Operating in the Nonequilibrium Conduction Mode," *Energy Conversion*, Vol. 9, No. 1, March 1969, pp. 13–23.

[11] Rouse, H., *Advanced Mechanics of Fluids*, Wiley, New York, 1959.

[12] Dicks, J. B. et al., "Diagonal Conducting Wall Generators," TR AFDAPL-TR-67-25, 1967, Air Force Aero Propulsion Lab., Wright-Patterson Air Force Base, Ohio.

[13] Frost, L. S., "Conductivity of Seeded Atmospheric Pressure Plasmas," *Journal of Applied Physics*, Vol. 32, No. 10, Oct. 1961, p. 2029.

[14] Bitiurin, V. A. et al., "A Study of Non-ideal MHD Generator Performance in the Presence of Hall Effect," *Proceedings of the 10th Symposium on Engineering Aspects of MHD*, Massachusetts Institute of Technology, Cambridge, Mass., March 1969.